



Mechanistic model of the *Escherichia coli* inactivation by solar disinfection based on the photo-generation of internal ROS and the photo-inactivation of enzymes: CAT and SOD

María Castro-Alfárez^{a,b}, María Inmaculada Polo-López^{a,b}, Javier Marugán^c, Pilar Fernández-Ibáñez^{a,b,*}

^a Plataforma Solar de Almería – CIEMAT, P.O. Box 22, 04200 Tabernas (Almería), Spain

^b CIESOL, Joint Centre of the University of Almería–CIEMAT, 04120 Almería, Spain

^c Department of Chemical and Environmental Technology, ESCET, Universidad Rey Juan Carlos, C/Tulipán s/n, 28933 Móstoles (Madrid), Spain

HIGHLIGHTS

- Mechanistic model for *E. coli* inactivation by solar disinfection is presented.
- Intracellular ROS attacks are proposed as the source of damage in bacteria.
- Defence mechanisms against oxidative stress (enzymes) is affected by solar radiation.
- Internal ROS formation and enzymes inactivation are promoted by photon action.
- CAT photo-inactivation kinetic constant is experimentally determined.

ARTICLE INFO

Article history:

Available online 23 June 2016

Keywords:

E. coli
SODIS
Mechanistic model
ROS-formation
SOD
Catalase

ABSTRACT

A mechanistic model of the inactivation of *Escherichia coli* by solar water disinfection (SODIS) technique is presented. Bacterial inactivation by SODIS is commonly attributed to the oxidative stress generated by synergy among solar radiation (UV photons) and mild temperature. Photons may increase the naturally occurring amount of internal Reactive Oxygen Species (ROS), such as hydroxyl radical (HO^\bullet) and superoxide radical (O_2^\bullet). ROS attacks to different targets inside the cells are one of the main sources of oxidative damage over cells. Besides, photons may damage the two essential enzymes of the defense system against intracellular oxidative stress, catalase (CAT) and superoxide dismutase (SOD). Therefore, the proposed model is a simplified approach of the complex processes occurring inside cells during SODIS, which is based on the photo-induced formation of intracellular ROS and the photo-inactivation of CAT and SOD. The model considers two individual volume units in which the processes are occurring simultaneously: (i) a single cell (mass balances for intracellular ROS and enzymes) and (ii) the reactor (mass balance for bacteria).

Kinetic constant from literature were used, meanwhile CAT photo-inactivation kinetic constant was determined experimentally, $(1.50 \pm 0.04) \cdot 10^7 \text{ cm}^3 \text{ Einstein}^{-1}$. Model regression was done using experimental data of *E. coli* inactivation by solar disinfection at different controlled conditions of solar irradiance and initial bacterial concentration. The good fit of the simulated and experimental results suggested that the mechanistic process proposed is a realistic approach of the disinfection process. Moreover, simulations of the time profile of intracellular ROS and enzymes involved during bacterial inactivation by SODIS are also presented.

© 2016 Elsevier B.V. All rights reserved.

1. Introduction

Solar water disinfection, commonly known as SODIS, is considered by the World Health Organization (WHO) an appropriate

* Corresponding author at: Plataforma Solar de Almería – CIEMAT, Ctra Senes, Km 4, 04200 Tabernas, Almería, Spain.

E-mail address: pilar.fernandez@psa.es (P. Fernández-Ibáñez).

household water treatment and storage (HWTS) intervention which has gained popularity in communities where access to standard sources of safe drinking water is a problem in the last decades [1]. It has been implanted successfully in diverse areas worldwide by several projects achieving a significant reduction in the number of waterborne diseases [2,3]. SODIS commonly refers to the water treatment that undergoes within PET (polyethylene terephthalate) bottles of 1.5–2 L that are exposed to sunlight

Nomenclature

SODIS	solar disinfection	κ^*	specific absorption coefficient ($\text{M}^{-1} \text{cm}^{-1}$)
ROS	reactive oxygen species	G	incident radiation ($\text{Einstein cm}^{-2} \text{s}^{-1}$)
CAT	catalase	I_{UVA}	incident radiation (W cm^{-2})
SOD	superoxide dismutase	E_p	photon energy (J photon^{-1})
NAD ⁺ /NADH	oxidized/reduced nicotinamide adenine dinucleotide	N_A	Avogadro number ($\text{photon Einstein}^{-1}$)
B	bacteria	NRMSLE	normalized root mean squared logarithmic error (%)
OM	organic matter		
CFU	colony forming units		
A_v	catalase volumetric specific activity ($\text{U/L} = \mu\text{mol H}_2\text{O}_2 \text{ min}^{-1} \text{L}^{-1}$)	Subscripts	
$\epsilon_{\text{H}_2\text{O}_2}$	extinction absorption coefficient of H_2O_2 ($\text{M}^{-1} \text{cm}^{-1}$)	0	indicates initial condition
l	optical length (cm)	V	relative to viable bacteria
k	kinetic constant (units depend on the specific reaction step)	I	relative to inactive bacteria
γ_1	kinetic parameter (M s^{-1})	Red	reduced
γ_2	kinetic parameter ($\text{M cm}^3 \text{Einstein}^{-1}$)	Ox	oxidized
γ_3	kinetic parameter (s^{-1})		
t	time (s)	Special symbols	
λ	wavelength (nm)	[]	concentration of intracellular chemical species (M) or concentration of bacteria in the bulk (CFU mL^{-1})
e^a , LVRPA	local volumetric rate of photon absorption ($\text{Einstein cm}^{-3} \text{s}^{-1}$)	–	indicates an averaged valued in the UVA range (300–400 nm)
κ	absorption coefficient (cm^{-1})		

during 6 h under clear sky conditions. The efficiency of SODIS to reduce the microbial load making drinking water safer has been widely demonstrated against several water pathogens, mainly for faecal bacteria (*Escherichia coli*, *Enterococcus fecalis*, *Vibrio cholera*, *Salmonella*, etc.) responsible for a number of enteric diseases (outbreaks, morbidity and mortality) [1].

The disinfection mechanism is considered a complex process with multi-steps acting simultaneously that result in the inactivation of the microorganisms. Firstly, it is accepted that UVB (280–320 nm) causes DNA damages resulting from the direct absorption of light that may stop DNA replication or generate mutations [4]. Solar UVB range radiation reaches the Earth's surface only in a low percentage (5% of UV range) due to the majority extraterrestrial UVB is absorbed by stratospheric ozone. Thus, in spite of being a direct source of intracellular injury UVB is not considered the main lethal agent for microorganisms in SODIS, but other mechanisms recognized that favor microbial inactivation are series of attacks of internal reactive oxygen species (ROS) induced by UVA range [5,6]. The formation of ROS occurs after light absorption by endogenous chromophores inside the cells. ROS are able to oxidize almost every compound in the cell that may lead to internal damages as the formation of pyrimidine dimers, the peroxidation of proteins and lipids, losses in membrane permeability or DNA rupture generating single strand breaks (SSBs) [7]. In addition, dissolved oxygen and natural dissolved organic matter in the water could induce photochemical reactions absorbing UV light that promote the formation of ROS in water, inducing a quicker bacterial inactivation. Aerobic microorganisms have a series of regulating processes to inhibit ROS action. Some enzymes as catalase (CAT), peroxidase or superoxide dismutase (SOD) act as scavenger of ROS against the photo-oxidative damage. Temperature also strongly affects the solar disinfection process inducing a synergetic effect with sunlight that shortens the treatment time with increased temperature values [8], but strongly when temperatures are above 45 °C [9].

The most used disinfection models are empirical equations based on Chick's law and its modifications to fit the different inactivation curves behavior (shoulders and tails) that were reviewed [10]. The mentioned work also reported some pseudo-mechanistic photo-catalyst models as lipid peroxidation mechanism, microbe-catalyst interaction models, series-event and multi-target models.

In the TiO_2 photo-catalytic disinfection field, additional efforts to model the mechanisms by which bacteria are inactivated were done [11,12]. Nevertheless, in literature there are no contributions focused on modelling intracellular reactions that lead to bacteria inactivation by SODIS. Some attempts to model it were previously reported [13,14], which developed stochastic models in which the complex intracellular processes are not considered. In this sense, it is necessary to couple the wide pool of biological information available on microorganisms and the kinetic models knowledge to develop a mechanistic model for the intracellular reactions taking place when bacterial suspensions are exposed to sunlight.

In the present work, a novel approach for the kinetic modelling of the SODIS process is presented. The model attempts to describe the mechanisms by which bacteria present in non-turbid water are inactivated when exposed to sunlight in a reasonably simplified way. The model considers that bacterial inactivation is mainly due to the oxidative stress of ROS generated under sunlight inside cells. It takes into account the intracellular reactions of generated ROS due to UVA range, specifically superoxide radicals (O_2^-), hydrogen peroxide (H_2O_2), hydroxyl radicals (HO^\bullet) and hydroperoxyl radicals (HO_2^\bullet) that depends on the intensity of radiation. The model also considers the photo-inactivation of CAT and SOD as part of the complex disinfection mechanisms of SODIS [6]. The kinetics of CAT photo-inactivation under solar radiation was experimentally determined through independent measurements in the same conditions of solar disinfection experiments and used as a known model parameter. The values for the rest of the model parameters were estimated using experimental data of bacterial concentration in clear water during solar disinfection experiments performed under controlled conditions of irradiance and temperature. The developed model is capable to predict the time profile of the species involved in the bacteria inactivation as the intracellular ROS and enzymes, and the bacteria concentration in water as well.

2. Experimental work

2.1. *E. coli* strains enumeration and quantification

E. coli strain K12 (CECT 4624) was obtained from the Spanish Culture Collection (CECT) and used for experiments in distilled

water spiked with seeded bacteria. Fresh liquid cultures were prepared in Luria-Bertani nutrient medium (LB Broth, Panreac) and incubated at 37 °C with rotary shaking for 20 h. The bacterial stationary phase concentration was 10^9 CFU mL⁻¹. Bacterial suspensions were harvested by centrifugation at 900g for 10 min. Bacterial pellet was re-suspended in phosphate-buffered saline (PBS) solution and diluted to different initial concentration depend on the experiment done. The samples taken during the experiments were enumerated using the standard plate counting method using Luria Bertani agar, through serial 10-fold dilutions in PBS. Colonies were counted after incubation for 24 h at 37 °C.

2.2. Measurement of CAT activity

CAT activity was measured in enzyme photo-inactivation experiments as the procedure described elsewhere [15]. Briefly, 100 mg/L of bovine liver catalase (Sigma-Aldrich, USA) was prepared in solution at 50 mM potassium buffer, pH 7.0, prepared as 4.08 g/L KH₂PO₄ and 3.48 g/L K₂HPO₄. Then it was diluted directly in the reactor to achieve a final concentration of 30 mg/L-CAT. Enzyme activity of the samples taken during the experiments was measured by the catalyzed decomposition of 50 mM H₂O₂ (prepared in 50 mM potassium buffer, pH 7.0) that were added to the samples of irradiated catalase. Absorbance at 240 nm was immediately monitored every 10 s to graph absorbance versus time and calculate the slope ($\Delta A_{240\text{nm}}/\text{min}$). Then the volumetric specific activity (A_v) of CAT expressed as U/L is obtained according to Eq. (1), where U is the unit of catalase activity that is equal to μmol of H₂O₂ decomposed by catalase per minute.

$$A_v \left(\frac{\text{U}}{\text{L}} \right) = \frac{\text{slope} \cdot 10^6}{\epsilon_{\text{H}_2\text{O}_2} \cdot l} \quad (1)$$

where the extinction absorption coefficient of H₂O₂ ($\epsilon_{\text{H}_2\text{O}_2}$) is equal to 43.6 M⁻¹ cm⁻¹ and the optical length (l) is given in terms of cm.

2.3. Solar experiments under controlled conditions

Two types of experiments were performed: (1) bacteria solar disinfection at different initial concentration and at different irradiances values and (2) photo-inactivation of catalase at different irradiance values. All experiments were conducted in a solar simulator (Atlas Suntest XLS+, USA) to be able to control irradiance conditions. It works with a xenon lamp and a combination of filters to simulate the solar global radiation outdoors spectrum. Experiments were performed in a stirred crystallizer of 19 cm of diameter which provides an irradiated surface of 0.0284 m² and where the whole volume was illuminated. The system is big enough to neglect radial profiles and consider a one-dimensional radiation gradient. Experiments were done in distilled water, with total volume of 700 mL. In solar disinfection experiments, a NaCl saline solution 0.9%w/v was used to avoid bacterial osmotic stress. Experiments were performed three times, and results were highly reproducible (>95% confidence level), average from the three replicates is showed in the graphs with error bars as the corresponding standard deviation. Temperature was monitored and it remained below 30 °C during all experiments, which was previously demonstrated that had no significant effect on the solar disinfection performance [1].

3. Modelling

3.1. Kinetic model

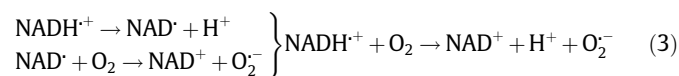
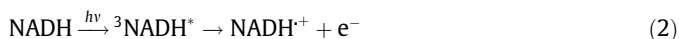
The proposed mechanism for the description of the SODIS process is based on three assumptions:

- (i) ROS are formed inside cells as a consequence of the biochemical routes of metabolism where oxygen plays an important role. Briefly, under aerobic conditions it could be considered that intracellular oxygen concentration is almost equivalent to extracellular oxygen [16]. O₂ acts as final acceptor of electrons in the so-called electron transport chain (ETC). It is the final and most important step of cellular respiration since the energy needed in the cell to conduct any activity is generated. During the ETC, several redox reactions occur and the electrons flux obtained from donor molecules such as NAD⁺, NADP⁺, flavoprotein, quinone or hemo groups will be used to generate energy which is stored in the cell as Adenosine TriPhosphate (ATP, energy-carrying molecule found in cells) [17]. Although redox process is conducted with high efficiency, a little percentage of free electrons interacts with the intracellular O₂ to reduce it prematurely to O₂⁻, and then to other ROS. Under sunlight radiation, the generation of O₂⁻ is increased by the excitation of some photosensitizers [18].
- (ii) Bacteria have a series of regulation mechanisms to control the toxic levels of ROS naturally formed inside cells. SOD reduces O₂⁻ to H₂O₂ and then CAT reduce H₂O₂ to water [19]. Nevertheless, solar radiation may alter the enzyme activity.
- (iii) The balance of the intracellular ROS and their regulation by enzymes is altered when bacterial suspensions are exposed to sunlight, leading to inactivation of bacterial cells through a process in which recovery by the cell defense mechanisms can also take place.

Rigorous description of all involved biochemical routes is far beyond the possibilities of the kinetic description of the global SODIS process. The proposed simplified model captures the essential steps of the global process, being considered as an optimal compromise between the fundamental description of the process and the simplicity model's requirements for engineering purposes. Table 1 summarizes the reaction steps considered in the mechanism (ROS formation, ROS recombination, enzymes photo-inactivation, etc.) that will be explained below.

3.1.1. Internal ROS formation

Under solar irradiation, the natural formation of ROS inside cells is accelerated by photosensitizers that are excited to high energy levels and donates an electron to oxygen, thus reducing it. Although there are several endogenous photosensitizers such flavins or quinons, NADH is one of the main photosensitizers that promotes the O₂⁻ formation from oxygen molecule [20]. It was previously reported the redox cycle NADH/NAD⁺ under UV exposure: (i) NADH is excited to ³NADH* that is quickly oxidized to NADH⁺, Eq. (2) (ii) NADH⁺ forms an intermediate compound, NAD[•], that in presence of oxygen, is oxidized to NAD⁺ reducing the oxygen to superoxide radical, Eq. (3) (iii) to complete the redox cycle, NAD[•] is again reduced to NADH, Eq. (4) [18,21].



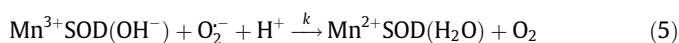
These reactions are the intermediate steps of the global reaction of superoxide formation induced by sunlight summarized in Eq. (T.2) [18]. This reaction and reaction Eq. (T.1), that occurs naturally during cell respiration process, are responsible for the formation of O₂⁻ in the cells when are exposed to sunlight.

Table 1Proposed mechanism for the solar water disinfection of *E. coli* based on the photo-generation of intracellular ROS and photo-inactivation of protective enzymes (CAT and SOD).

Step	Reaction	Rate	Kinetic constant value
Internal ROS formation	$O_2 + e^- \longrightarrow O_2^-$	Eq. (T.1)	$k_1[O_2][e^-]$
	$O_2 + e^- \xrightarrow{h\nu, NADH} O_2^-$	Eq. (T.2)	$k_2[O_2][e^-]e_{NADH}^a$
	$O_2^- + H^+ \xrightarrow{SOD} \frac{1}{2}H_2O_2 + \frac{1}{2}O_2$	Eq. (T.3)	$k_3[O_2^-][SOD]$
	$Fe^{2+} + H_2O_2 \longrightarrow Fe^{3+} + HO^- + HO^\bullet$	Eq. (T.4)	$k_4[Fe^{2+}][H_2O_2]$
	$Fe^{3+} + H_2O \xrightarrow{h\nu} Fe^{2+} + HO^\bullet + H^+$	Eq. (T.5)	$k_5[Fe^{3+}][H_2O]e_{Fe^{3+}}^a$
ROS recombination	$H_2O_2 + HO^\bullet \longrightarrow HO_2 + H_2O$	Eq. (T.6)	$k_6[H_2O_2][HO^\bullet]$
	$HO_2 \longrightarrow \frac{1}{2}H_2O_2 + \frac{1}{2}O_2$	Eq. (T.7)	$k_7[HO_2]^2$
H_2O_2 decomposition	$H_2O_2 \xrightarrow{CAT} \frac{1}{2}O_2 + H_2O$	Eq. (T.8)	$k_8[H_2O_2][CAT]$
Enzymes photo-inactivation	$CAT \xrightarrow{h\nu} CAT_i$	Eq. (T.9)	$k_9[CAT]e_{CAT}^a$
	$SOD \xrightarrow{h\nu} SOD_i$	Eq. (T.10)	$k_{10}[SOD]e_{SOD}^a$
Cell damages caused by ROS	$OM_{red} + HO^\bullet \longrightarrow OM_{ox}$	Eq. (T.11)	$k_{11}[HO^\bullet]$
	$OM_{red} + O_2^- \longrightarrow OM_{ox}$	Eq. (T.12)	$k_{12}[O_2^-]$
Bacteria inactivation	$B_v \xrightarrow{HO^\bullet, O_2^-} B_i$	Eq. (T.13)	$k_{13}[HO^\bullet][O_2^-][B_v]$

 B_v : viable bacteria. B_i : inactivated bacteria. OM_{red} : organic matter reduced. OM_{ox} : organic matter oxidized. e_{NADH}^a : local volumetric rate of photon absorption of NADH. $e_{Fe^{3+}}^a$: local volumetric rate of photon absorption of Fe^{3+} . e_{CAT}^a : local volumetric rate of photon absorption of CAT. e_{SOD}^a : local volumetric rate of photon absorption of SOD.

Imlay and co-workers studied the natural generation of intracellular O_2^- in *E. coli* and determined that the reaction rate of Eq. (T.1) is 5 $\mu M/s$ [16,22]. Nevertheless, the concentration of this radical at steady state was found to be significantly low ($10^{-10} M$) due to the action of SOD, which transforms it into H_2O_2 in the presence of H^+ , Eq. (T.3). *E. coli* contains two cytoplasmic SOD enzymes, manganese- and iron-cofactored types (MnSOD and FeSOD) and a single periplasmic SOD enzyme, copper, zinc-cofactored type (CuZnSOD) [19]. Viglino and co-workers studied the kinetics of CuSOD reaction [23] and then other researchers completed the mechanism of SOD by the observation of a burst phase and a zero-order phase in MnSOD [24]. The proposed mechanism was expressed by the redox cycle of the Mn cofactor Eqs. (5) and (6).



where k and k' are the kinetic constants of each semi-reaction. The resulting reaction is expressed as Eq. (T.3) which kinetic constant is considered the equivalent of the limiting reaction. The cytoplasmic SOD concentration in *E. coli* was determined to be 20 μM [19].

Intracellular H_2O_2 generates hydroxyl radical (HO^\bullet) by Fenton like reactions Eqs. (T.4) and (T.5), that is the one of the species that can directly damage most biomolecules [19]. Iron takes part in these reactions as a catalyst due to Fe^{2+} is oxidized to Fe^{3+} and then reduced again to its initial state. The reduction of iron is a spontaneous reaction that is accelerated by UV and visible light becoming Eq. (T.4) the limiting reaction of the internal photo-Fenton process. The iron that catalyzes these reactions is called “free iron” referring to the iron that is not incorporated into enzymes or iron-storage proteins. Bound iron can be released from enzyme co-factors such iron-sulfur cluster by ROS, specifically by superoxide radicals or hydrogen peroxide, or even from nucleic acids, proteins and lipids. *E. coli* contains approximately 20 μM of Fenton-active ferrous iron [25].

Due to the high reactivity of ROS, several ROS recombination reactions happen. Contributions from Buxton, Gallard and co-workers collect a large list of ROS reactions [26,27]. From the

kinetics point of view Eqs. (T.6) and (T.7) are two of the most representative ROS recombination reactions that have been used in other photo-oxidative models [28,29].

3.1.2. H_2O_2 decomposition

SOD controls the concentration of O_2^- at low levels in natural conditions, nevertheless it also generates H_2O_2 at a rate of 15 $\mu M/s$ [17]. Taking into account that levels above 1 μM are substantially toxic [19], cells require a defensive mechanism against H_2O_2 . In most of the microorganisms H_2O_2 is scavenged by peroxidases and catalase. The primary scavenger in *E. coli* is the alkylhydroperoxide reductase (Ahp) that is so effective that the concentration of H_2O_2 at the steady-state does not exceed 20 nM [19]. Nevertheless, levels of H_2O_2 higher than 100 nM cause the activity of Ahp to top out. Then catalase is strongly induced, becoming the primary scavenging enzyme.

When bacterial suspension is exposed to UV radiation, H_2O_2 content is expected to be higher than 100 nM so that catalase is considered the primary scavenging enzyme while Ahp action is neglected. The decomposition mechanism of H_2O_2 by catalase is a very complex process that is not known in complete detail due to the variety of interactions between catalase and H_2O_2 , HO^\bullet and HO_2 [30]. In this work, we have considered a simplified mechanism, one of the most accepted, where Fe^{3+} is serving as electron source forming an Fe-intermediate [31]:



where k and k' are the kinetic rate constants of each semi-reaction. The resulting reaction is expressed as Eq. (T.8), whose kinetic rate constant is considered the same as that limiting reaction. Catalase at steady-state in *E. coli* was determined as 92 μM [32,33]. Alternative mechanisms considering the presence of iron traces are also reported in the literature, where catalase reaction with H_2O_2 was modeled as a generalized uncompetitive inhibition Yano-Koya [34].

3.1.3. Enzymes inactivation by UV light action

Enzymes are also affected by solar light [35,36]. SOD and CAT are macromolecular biological catalysts whose activity decreases under the action of UV radiation. Moreover, the concentration of intracellular ROS, such as O_2^- and H_2O_2 , may change during the solar exposure of bacteria cells. Eqs. (T.9) and (T.10) represent the photo-inactivation of both enzymes. Bosshard and co-workers found evidences of the reduction of catalase activity during SODIS treatment [37]. To our knowledge there is not any reported research of the photo-inactivation kinetics of these enzymes. In this study, photo-inactivation of catalase was experimentally evaluated under the same conditions of solar disinfection tests, to determine the kinetic parameter of Eq. (T.9).

3.1.4. Internal oxidative damages that lead into cells inactivation

Generally, ROS are capable to oxidize the organic matter and constituent components in cells. Scientific community agreed that all the reactive species whose formation is photo-induced by near UV are source of injury and the precursors of the cell inactivation. Nevertheless, there is no experimental evidence that identify ROS as main responsible for solar disinfection, although the most commonly attributed species are hydroxyl radicals, superoxide radicals, hydrogen peroxide and singlet oxygen [1,5,38]. A complete solar water disinfection model should include all ROS that could oxidize cells components and lead to the disruption of the cellular metabolism and to a later cell inactivation. This simplified model considers only the two ROS more oxidative as a simplification of the several existing sources of intracellular oxidative stress. Eqs. (T.11) and (T.12) refer those attacks to several intracellular targets that are encompassed in the term OM_{red} as the organic matter that is susceptible to be oxidized by HO^\bullet or O_2^- .

Proteins can be the main target of ROS during SODIS due to an increase in protein carboxylation at the first stage of irradiation [37], this can be followed by an accumulation of proteins' aggregates after longer periods of irradiation. The proteins that are damaged during solar exposure are enzymes involved in translation, transport, transcription, glycolysis, DNA-repair, respiration, protein folding and ATP synthesis [39]. In general, the accumulation of several damages by ROS is necessary to achieve cell death, and the bacteria with intermediate levels of damage would be still able to growth in a suitable culture medium or specific growth conditions. The macroscopic reaction of bacterial inactivation can be considered as activated or mediated by the intracellular ROS according to Eq. (T.13). Therefore, the mass balance of viable bacteria could be expressed in terms of the concentration of bacteria in water and the reaction rate is dependent on the intracellular concentrations of HO^\bullet and O_2^- (see Table 1). The units of the apparent kinetic constant k_{13} are $M^{-2} s^{-1}$ that are referred to the bacterial cell volume, while the reaction rate of the bacteria inactivation ($d[B_v]/dt = -k_{13}[HO^\bullet][O_2^-][B_v]$) is expressed in terms of $CFU mL^{-1} s^{-1}$ referred to the reactor volume.

Mass balance for each species involved in the process can be solved for a single cell volume (details in the Appendix) to obtain the profiles of concentration of ROS and enzymes versus the treatment time. Mass balance of bacteria in the whole reactor volume was also determined (Appendix). The final expressions for calculating the concentration of each compound inside a bacteria cell and the bacteria concentration in the reactor at the instant time t are:

$$\frac{d[B_v]_t}{dt} = -k_{13} \cdot \frac{2\gamma_3[H_2O_2]_t}{k_6[H_2O_2]_t + k_{11}} \cdot \frac{\gamma_1 + \gamma_2 \cdot e^a_{NADH}}{k_3[SOD]_t + k_{12}} \cdot [B_v]_t \quad (9)$$

$$\frac{d[H_2O_2]_t}{dt} = \frac{1}{2} \cdot \frac{k_3[SOD]_t(\gamma_1 + \gamma_2 \cdot e^a_{NADH})}{k_3[SOD]_t + k_{12}} - \frac{\gamma_3 \cdot k_6[H_2O_2]_t^2}{k_{11} + k_6[H_2O_2]_t} - (\gamma_3 + k_8[CAT]_t)[H_2O_2]_t \quad (10)$$

$$[O_2^-]_t = \frac{\gamma_1 + \gamma_2 \cdot e^a_{NADH}}{k_3[SOD]_t + k_{12}} \quad (11)$$

$$[HO^\bullet]_t = \frac{2\gamma_3[H_2O_2]_t}{k_6[H_2O_2]_t + k_{11}} \quad (12)$$

$$[HO_2]_t = \sqrt{\frac{k_6}{k_7} [H_2O_2]_t [HO^\bullet]_t} \quad (13)$$

$$[CAT]_t = \frac{1}{1/[CAT]_0 + k_9 \cdot \bar{\kappa}_{CAT} \cdot \bar{G} \cdot t} \quad (14)$$

$$[SOD]_t = \frac{1}{1/[SOD]_0 + k_{10} \cdot \bar{\kappa}_{SOD} \cdot \bar{G} \cdot t} \quad (15)$$

$$\text{being } \gamma_1 = k_1[O_2]_t[e^-]_t, \gamma_2 = k_2[O_2]_t[e^-]_t \text{ and } \gamma_3 = k_4[Fe^{2+}]_t \quad (16)$$

where $[B_v]_t$ is the concentration of viable bacteria in the reactor at the instant time t , $[HO^\bullet]_t$, $[O_2^-]_t$, $[HO_2]_t$, $[H_2O_2]_t$, $[CAT]_t$, $[SOD]_t$, $[O_2]_t$, $[e^-]_t$, $[Fe^{2+}]_t$ are the concentration of each species at the instant t , $[CAT]_0$, $[SOD]_0$ are the initial enzymes concentrations and e^a , $\bar{\kappa}$, \bar{G} are light dependant parameters that are explained below.

3.2. Light dependence parameters: definition and calculation

To estimate the parameters of the model it is necessary to evaluate the absorption of light of some species (CAT, SOD and NADH) in the reactor. The reactor chosen to run the experiments has a diameter big enough to consider a one-dimensional light transport. Considering the low optical density of the system, the reactor can be considered to be working under optically differential conditions, and given the characteristics of the reactor and solar simulator lamp, the local volumetric rate of photon absorption of each compound (LVRPA, e^a) can be considered constant in the entire photo-reactor. Assuming that optical properties of bacteria are constant during the treatment, LVRPA can be also considered constant with time. e^a values for each compound can be estimated using the following equation.

$$e^a_i = \int_{\lambda_1}^{\lambda_2} \kappa_{\lambda,i} \cdot G_\lambda d\lambda \quad (17)$$

where $\kappa_{\lambda,i}$ is the absorption coefficient of the compound i at λ wavelength in terms of cm^{-1} , and G_λ is the incident radiation at λ wavelength in terms of Einstein $cm^{-2} s^{-1}$. The estimation of these parameters was done as an approximation using the averaged value in the UVA range (300–400 nm), $\bar{\kappa}_i$ and \bar{G} . Further work to improve this model will consider different parts of the spectrum, including UVB and visible ranges. $\bar{\kappa}_i$ was determined as the product of specific absorption coefficient averaged in the UVA range $\bar{\kappa}_i^*$ and the concentration of the compound i , $[i]$:

$$\bar{\kappa}_i = \bar{\kappa}_i^* \cdot [i] \quad (18)$$

$\bar{\kappa}_{CAT}^*$ was experimentally determined as $2.6 \cdot 10^5 M^{-1} cm^{-1}$, $\bar{\kappa}_{SOD}^*$ and $\bar{\kappa}_{NADH}^*$ were obtained from literature [40,41]. CAT and SOD concentrations vary with treatment time (see Appendix) and NADH concentration was considered constant at the basal concentration in *E. coli* [42]. \bar{G} could be estimated from the incident UVA radiation programmed in the solar simulator I_{UVA} , in terms of $W cm^{-2}$, the photon energy averaged in the UVA range \bar{E}_p (J photon $^{-1}$) and the Avogadro number N_A (photon Einstein $^{-1}$):

$$\bar{G} = \frac{I_{UVA}}{\bar{E}_p \cdot N_A} \quad (19)$$

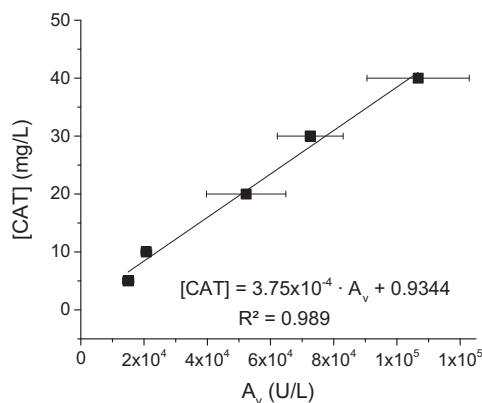


Fig. 1. Correlation of the catalase concentration [CAT] and its volumetric activity A_v , in the range of 5–40 mg/L. Deviation standard of A_v is represented by error bars.

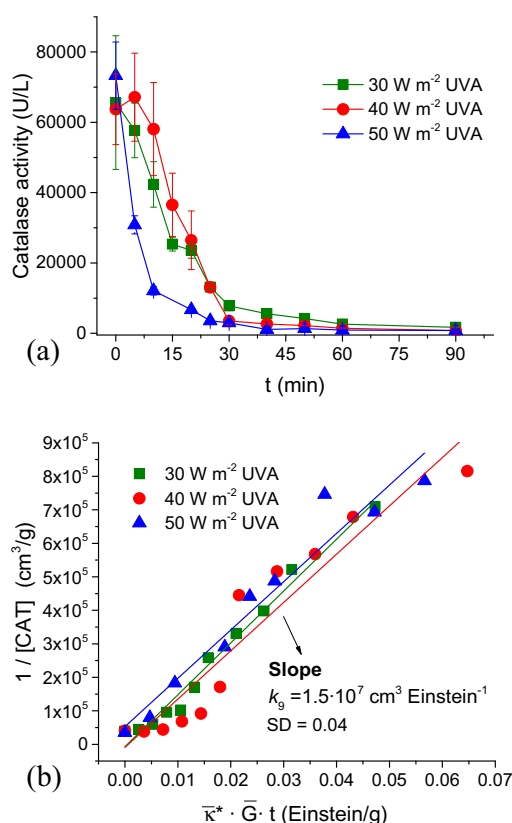


Fig. 2. (a) Photo-inactivation of catalase enzyme in distilled water at 30, 40 and 50 W m^{-2} of UVA (dots) and (b) regression by least squares method to determine the kinetic constant parameter (lines).

3.3. Estimation of model parameters

The model is able to predict the concentration of bacteria over the treatment time by solving Eq. (9) applied to the whole water volume reactor. This differential equation must be solved simultaneously to other equations of the model, Eqs. (10)–(15), as they have common variables. Those equations are applied to one single cell and consisted on the set of equations in Table 1. According to the isotropic hypothesis, the same internal reactions will occur in all cells without population, time or space preferences. Consequently, intracellular species involved in the process are behaving similar in all cells. These coupled system of equations was solved using the Dormand-Prince method, briefly is a Runge-Kutta method for fourth and fifth order solution.

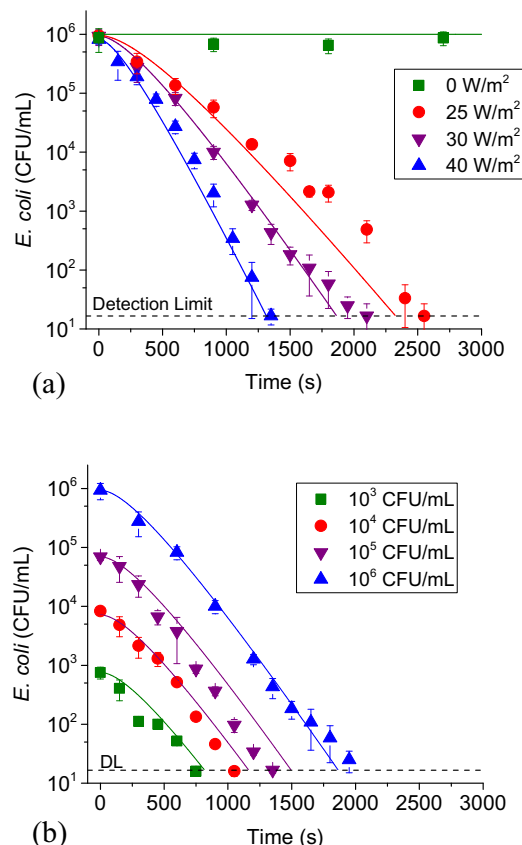


Fig. 3. Inactivation of *E. coli* by solar disinfection. Comparison between experimental data (dots) and modeled data (lines) at (a) an initial concentration of 10^6 CFU mL^{-1} and 0, 25, 30, 40 W m^{-2} UVA irradiances and (b) 30 W m^{-2} and 10^3 , 10^4 , 10^5 , 10^6 CFU mL^{-1} of initial bacteria concentration.

The model presented in this work has 13 kinetic parameters. Most of them have been previously studied by other authors and reported in literature as shown in Table 1. In some cases, the conditions for determining these kinetic constants are different from those found in the inner bacteria. Nevertheless, these differences may not be significant due to the species involved are most of them chemical compounds or biomolecules (CAT and SOD) that have been studied and reported *in vivo* in the literature. The kinetic constant of reaction Eq. (T.9), referring to the reduction of catalase activity due to the light action, has been determined experimentally in this work as explained below.

The model proposed finally has five unknown parameters: γ_2 (related with photo-generation of O_2^-), k_{10} (kinetic constant of SOD photo-inactivation), k_{11} (kinetic constant of cell's content oxidation by HO^\bullet), k_{12} (kinetic constant of cell's content oxidation by O_2^-) and k_{13} (kinetic constant of bacteria inactivation). The regression of the model was solved using MATLAB[®] software by the interior-point algorithm. The initial values of the parameters were searched by a Monte Carlo approach. The regression was run minimizing the normalized root mean squared logarithmic error (NRMSLE) of the experimental and predicted viable bacteria concentration.

4. Results and discussion

4.1. Catalase solar photo-inactivation

Previous tests on photo-inactivation experiments determined that the range of catalase concentration in which the activity measurement is reliable is between 3 and 50 mg/L. The reaction of

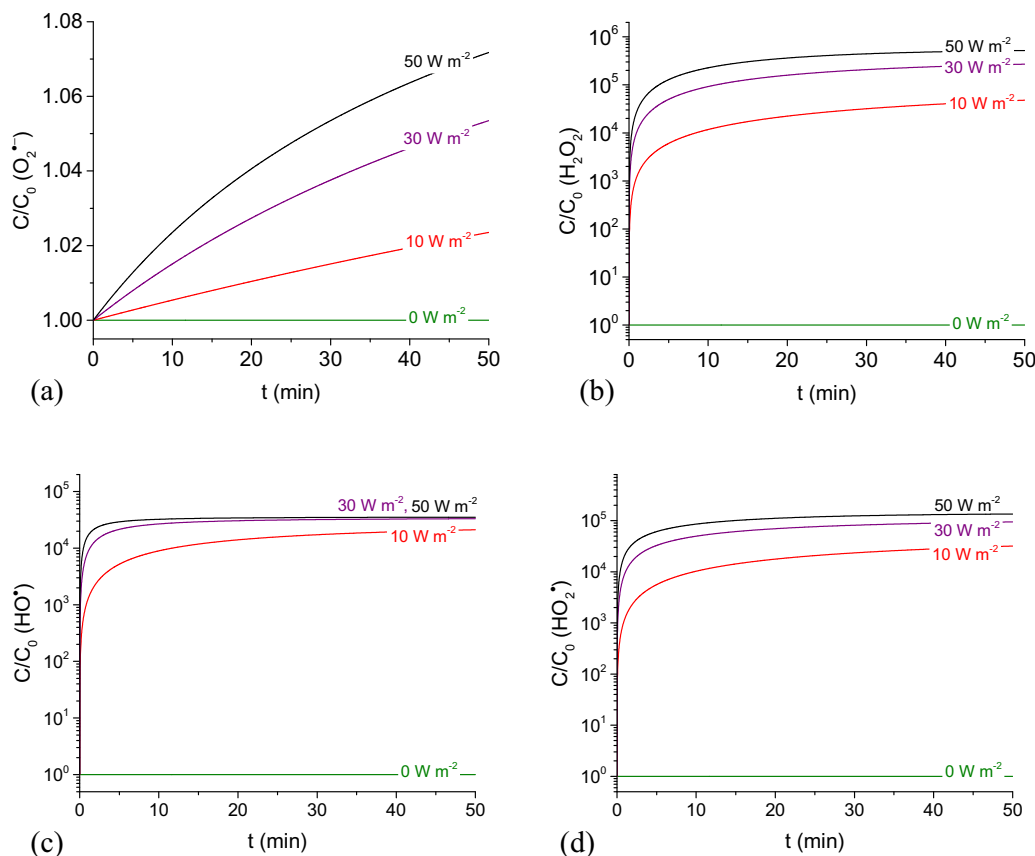


Fig. 4. Model simulations of the time-profile of intracellular (a) O_2^- , (b) H_2O_2 , (c) HO^\cdot and (d) HO_2 in *E. coli* during 50 min of solar water disinfection at 0, 10, 30 and 50 $W m^{-2}$ of UVA irradiances.

50 mM- H_2O_2 with added CAT at concentrations higher than 30 mg/L generated oxygen bubbles so quickly that absorbance measurements were considered unreliable. The detection limit for CAT concentration was 3 mg/L, below that value the reaction is too slow so that the activity of CAT couldn't be measured. CAT activity was measured using different concentrations (5, 10, 20, 30 and 40 mg/L) with the aim to obtain a correlation between activity and concentration, as presented in Fig. 1. Linear regression of experimental data permitted to determine the concentration of CAT (mg/L) equivalent to a specific activity of the enzyme (U/L).

Solar irradiated catalase experiments demonstrated that its activity was reduced when exposed to sunlight. Fig. 2(a) shows the decrease of catalase activity under different irradiances values (30, 40 and 50 $W m^{-2}$ of UVA). Photo-inactivation of CAT followed a first order kinetics with respect to CAT concentration and LVRPA according to Eq. (20).

$$r_{CAT} = k_9 [CAT] e_{CAT}^a \quad (20)$$

Although CAT activity was affected by solar exposure, the concentration of CAT did not change along radiation time. Therefore, [CAT] can be considered as the concentration of the "active catalase" in Eq. (20). This concentration can be estimated by the correlation curve between CAT-concentration and CAT-activity (Fig. 1).

Using the expression of LVRPA Eqs. (17) and (18) and integrating from time $t = 0$ (initial concentration of catalase, $[CAT]_0$) to a time t ([CAT]):

$$\frac{1}{[CAT]} = \frac{1}{[CAT]_0} + k_9 \cdot \bar{K}_{CAT}^* \cdot \bar{G} \cdot t \quad (21)$$

Eq. (21) gives the expression of the linear equation, whose slope is equal to the kinetic constant of CAT photo-inactivation Eq. (T.9). Fig. 2(b) shows the linear fits of the three experiments at different irradiance values and the regression by least squares method of the experimental data. The value of k_9 is resulted to be $1.5 \cdot 10^7 \text{ cm}^3 \text{ Einstein}^{-1}$.

4.2. Estimation of kinetics parameters

Solar disinfection experiments were performed at different operational conditions: initial bacteria concentration and irradiance values. The results showed (see Fig. 3), as expected, the higher dose intensity of radiation the faster bacterial inactivation; the initial concentration of bacteria does not affect to the kinetic constants. Experimental results were used for determining the model parameters by mathematical correlation between model predicted values and experimental data. Values obtained for these parameters and the NRMSLE are:

$$\begin{aligned} \gamma_2 &= 1.14 \cdot 10^5 \text{ M cm}^3 \text{ Einstein}^{-1} \\ k_{10} &= 1.56 \cdot 10^6 \text{ cm}^3 \text{ Einstein}^{-1} \\ k_{11} &= 2.04 \cdot 10^4 \text{ s}^{-1} \\ k_{12} &= 1.36 \cdot 10^5 \text{ s}^{-1} \\ k_{13} &= 8.03 \cdot 10^{15} \text{ M}^{-2} \text{ s}^{-1} \\ \text{NRMSLE} &= 8.32\% \end{aligned}$$

Fig. 3 shows the experimental and simulated results in the different conditions. This evidences that predicted results from the model and the optimized parameters fit satisfactorily experimental results. Even, the NRMSLE calculated for all the experiments is smaller than 10 %, which according to other works [43] can be considered an excellent regression.

It is important to note that parameters' values obtained in this work are specifically estimated for the operational conditions of the experiments done. In this sense, the kinetic parameters k_{11} , k_{12} and k_{13} were estimated using the common *E. coli* strain K12 in stationary phase. For other microorganism or other growth state of this bacterium, the parameters could be quite different and should be estimated for the specific cell and operational conditions. Furthermore, reactor setup is also an important factor due to it determines the inlet UV photon flux inside bacterial cells. Consequently, the kinetic values estimated could be applied for reactors with similar photon distribution than the used in this work.

The present model is the first simplified mechanistic SODIS model focused on the effect of solar UVA. Nevertheless, UVB and even visible range may be involved in the cell injury by different mechanisms and could lead to cell inactivation [6,35]. The first one is a direct source of DNA damage, while the second is expected to have a significant role in bacteria inactivation although is less energetic than UV. In addition, further modifications of this first model would include the effects of UVB, visible, and other important parameters such as temperature and water physicochemical characteristics, mainly the organic matter and natural photosensitizers, and water turbidity, that makes depletion in light absorbance.

4.3. Model predicted profiles of intracellular ROS and enzymes

This model is able to simulate and predict the time profile of intracellular ROS during solar water disinfection. The proposed species involved in the process are O_2^- , H_2O_2 , HO^\bullet and HO_2^\bullet . The

hypothesis done for mass balance equations of these species was that all the short lifetime radicals reach a micro stationary-state due to the high reactivity of the species, while H_2O_2 was considered in a non-stationary-state with possible accumulation. Simulation runs at different irradiance values are shown in Fig. 4. The simulation results predicted that H_2O_2 , HO^\bullet and HO_2^\bullet reach a new stationary-state in less than 10 min and increased their concentration up to 3-log even for 10 W m^{-2} . The simulated behavior of O_2^- is apparently quite different, as a very slight increase is observed in all cases, even for high irradiance as 50 W m^{-2} . Still, this increase is 5 orders of magnitude lower than the rest of ROS species (Fig. 4b–d). At view of these predictions, we can assume that the new stationary state for O_2^- is reached much faster than the others, so fast that the plateau profile of the other graphs is not observed here. This is a result of the high reaction rates for O_2^- consumption in the model. This is concordance with the low relevant role of the photo-inactivation reaction of SOD, as shown by its low kinetic rate constant ($k_{10} = 1.56 \cdot 10^6\text{ cm}^3\text{ Einstein}^{-1}$) as compared to the corresponding to catalase (k_9).

To our knowledge, this work is the first attempt to estimate the effect of ROS on the inactivation and how their concentrations vary during the process. Since there is not any experimental evidence of the evolution of these species during the process, ROS simulation results cannot be compared or validated with literature data. In this sense, intracellular ROS detection, that is a common technique in other fields such as the photodynamic therapy (PDT) [44], could be used for solar irradiated bacteria to better understand the SODIS process and confirm experimentally the role of ROS in this process. Nevertheless, PDT has developed for study ROS activity inside eukaryotic cells instead of prokaryotic due to its direct applications for medicine like cancer therapy. In line with this, further experimental investigations should be done to experimentally detect ROS in solar irradiated bacteria.

On the other hand, enzymes CAT and SOD are also involved in the bacteria inactivation. The SOD enzyme role in the protective mechanism during the solar irradiation was previously studied with *sodA sodB* mutants *E. coli* [45]. It was observed that the inactivation in the *E. coli* strain lack of SOD enzyme was faster than the wild type. Simulation profiles for CAT and SOD at different solar irradiances are shown in Fig. 5. Experimental data of CAT photo-inactivation are also presented (Fig. 5(a)) and it is observed that model fits accurately the experimental data obtained in the same experimental conditions. Simulations of both enzymes show, as expected, a reduction of their activity during the process. Nevertheless, SOD activity reduction is not as rapid as CAT. These simulations are in agreement with results obtained by other researchers [35] that studied experimentally the effect of UVA in enzyme levels of *E. coli* in seawater. In addition, the slow SOD activity decrease permits to control the amounts of O_2^- forming inside the cells. This fact is observed in the Fig. 4(a) where O_2^- profiles show a very slight increase even at 50 W m^{-2} .

5. Conclusions

The model presented in this work is the first attempt to summarize the main reactions that validate mathematically experimental evidence of *E. coli* inactivation due to the solar incidence. The model is successfully able to reproduce the time profile of the concentration of viable bacteria in clear water under different irradiances and different initial bacterial concentrations with a normalized root mean square logarithmic error of 8.32%. The mechanistic model is also capable to simulate the evolution of intracellular ROS and enzymes during SODIS.

The novelty of this model is the intracellular bacterial reactions proposed that occur in parallel during *E. coli* inactivation and the

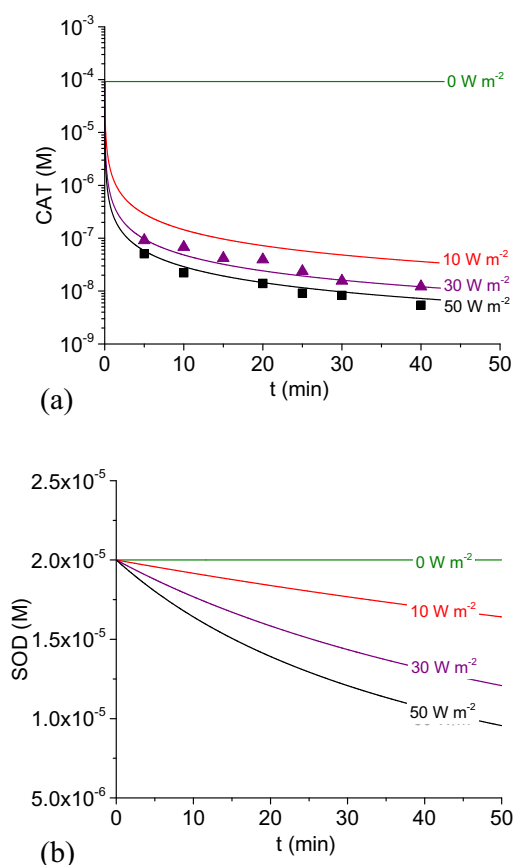


Fig. 5. Model simulations of the time-profile of intracellular (a) CAT (lines) and (b) SOD in *E. coli* during 50 min of solar disinfection at 0, 10, 30 and 50 W m^{-2} of UVA irradiances. Dots in (a) represent experimental data of CAT photo-inactivation at 30 W m^{-2} (▲) and 50 W m^{-2} (■).

kinetic parameters estimation of those reactions. Among this, bacterial inactivation is introduced in the model as a reaction mediated by intracellular HO^\bullet and O_2^- ($k_{13} = 8.03 \cdot 10^{15} \text{ M}^{-2} \text{ s}^{-1}$). Inside the cells, those attacks have been represented by the oxidation of natural organic matter by HO^\bullet and O_2^- ($k_{11} = 2.04 \cdot 10^4 \text{ s}^{-1}$ and $k_{12} = 1.36 \cdot 10^5 \text{ s}^{-1}$, respectively). Kinetic of the naturally formation of intracellular ROS was previously studied by other researchers but this work is the first attempt to determine the kinetic of the ROS formation due to the UVA photons action. The photo-generation of O_2^- is proposed as a reaction mediated by the natural photosensitizer NADH ($\gamma_2 = 1.14 \cdot 10^5 \text{ M cm}^3 \text{ Einstein}^{-1}$). Kinetic constant of CAT photo-inactivation was experimentally determined ($k_9 = 1.5 \cdot 10^7 \text{ cm}^3 \text{ Einstein}^{-1}$) and kinetic constant of SOD photo-inactivation was obtained by model regression ($k_{10} = 1.56 \cdot 10^6 \text{ cm}^3 \text{ Einstein}^{-1}$).

The reported model could be considered as an intrinsic kinetic description of the solar water disinfection process and the kinetic parameters could be applied for *E. coli* strain K12 and for reactors with similar photon flux distribution.

Acknowledgements

The authors wish to thank the Spanish Ministry of Economy and Competitiveness (MINECO) for financing this research through the collaborative WATER4FOOD (CTQ2014-54563-C3). The authors wish also to thank the financial support of the European project WATERSPOUTT H2020-Water-5c-2015 (GA 688928).

Appendix. Kinetic modelling

The reactions that modified the concentration of ROS inside bacterial cells by solar water treatment are summarized in Table 1. By applying the kinetic micro steady-state approximation for concentration of iron (Fe^{2+} and Fe^{3+}) and radicals (O_2^- , HO^\bullet and HO_2) inside a bacterial cell, and assuming that iron released from cluster due to oxidative stress is neglected, free iron has been considered constant during the process, the profiles of concentration in a single cell are derived:

Iron balances in a single cell:

$$\frac{d[\text{Fe}^{2+}]}{dt} = -\frac{d[\text{Fe}^{3+}]}{dt} = -k_4[\text{Fe}^{2+}][\text{H}_2\text{O}_2] + k_5[\text{Fe}^{3+}][\text{H}_2\text{O}]e_{\text{Fe}^{3+}}^a \approx 0 \quad (\text{A.1})$$

$$k_4[\text{Fe}^{2+}][\text{H}_2\text{O}_2] = k_5[\text{Fe}^{3+}][\text{H}_2\text{O}]e_{\text{Fe}^{3+}}^a \quad (\text{A.2})$$

Superoxide radicals balance in a single cell:

$$\frac{d[\text{O}_2^-]}{dt} = k_1[\text{O}_2][e^-] + k_2[\text{O}_2][e^-]e_{\text{NADH}}^a - k_3[\text{O}_2^-][\text{SOD}] - k_{12}[\text{O}_2^-] \approx 0 \quad (\text{A.3})$$

$$[\text{O}_2^-] = \frac{\gamma_1 + \gamma_2 \cdot e_{\text{NADH}}^a}{k_3[\text{SOD}] + k_{12}} \quad (\text{A.4})$$

Hydroxyl radicals balance in a single cell:

$$\frac{d[\text{HO}^\bullet]}{dt} = -k_6[\text{H}_2\text{O}_2][\text{HO}^\bullet] - k_{11}[\text{HO}^\bullet] + k_4[\text{Fe}^{2+}][\text{H}_2\text{O}_2] + k_5[\text{Fe}^{3+}][\text{H}_2\text{O}]e_{\text{Fe}^{3+}}^a \approx 0 \quad (\text{A.5})$$

$$[\text{HO}^\bullet] = \frac{2\gamma_3[\text{H}_2\text{O}_2]}{k_6[\text{H}_2\text{O}_2] + k_{11}} \quad (\text{A.6})$$

Hydroperoxyl radicals balance in a single cell:

$$\frac{d[\text{HO}_2]}{dt} = k_6[\text{H}_2\text{O}_2][\text{HO}^\bullet] - k_7[\text{HO}_2]^2 \approx 0 \quad (\text{A.7})$$

$$[\text{HO}_2] = \sqrt{\frac{k_6}{k_7}[\text{H}_2\text{O}_2][\text{HO}^\bullet]} \quad (\text{A.8})$$

where

$$\gamma_1 = k_1[\text{O}_2][e^-], \gamma_2 = k_2[\text{O}_2][e^-] \text{ and } \gamma_3 = k_4[\text{Fe}^{2+}] \quad (\text{A.9})$$

Hydrogen peroxide is a compound that cannot be considered in a micro steady state inside the bacterial cell. The rate expression of H_2O_2 is obtained by:

$$\frac{d[\text{H}_2\text{O}_2]}{dt} = \frac{1}{2}k_3[\text{O}_2^-][\text{SOD}] + \frac{1}{2}k_7[\text{HO}_2]^2 - k_4[\text{Fe}^{2+}][\text{H}_2\text{O}_2] - k_6[\text{H}_2\text{O}_2][\text{HO}^\bullet] - k_8[\text{H}_2\text{O}_2][\text{CAT}] \quad (\text{A.10})$$

Introducing Eqs. (A.4), (A.6) and (A.8) into Eq. (A.10), the hydrogen peroxide rate results to be:

$$\frac{d[\text{H}_2\text{O}_2]}{dt} = \frac{1}{2} \cdot \frac{k_3[\text{SOD}](\gamma_1 + \gamma_2 \cdot e_{\text{NADH}}^a)}{k_3[\text{SOD}] + k_{12}} - \frac{\gamma_3 \cdot k_6[\text{H}_2\text{O}_2]^2}{k_6[\text{H}_2\text{O}_2] + k_{11}} - (\gamma_3 + k_8[\text{CAT}])[\text{H}_2\text{O}_2] \quad (\text{A.11})$$

Enzymes are inactivated along treatment time due to the photon action. Among this, CAT and SOD are species in not-steady state:

$$\frac{d[\text{CAT}]}{dt} = -k_9[\text{CAT}]e_{\text{CAT}}^a \neq 0 \quad (\text{A.12})$$

$$\frac{d[\text{SOD}]}{dt} = -k_{10}[\text{SOD}]e_{\text{SOD}}^a \neq 0 \quad (\text{A.13})$$

Introducing the expression of LVRPA of each compound determined by Eqs. (17) into (A.12) and (A.13) and taking into account Eq. (18) for the calculation of the absorption coefficient, the following expressions are obtained:

$$\frac{d[\text{CAT}]}{dt} = -k_9 \cdot \bar{\kappa}_{\text{CAT}}^* \cdot \bar{G} \cdot [\text{CAT}]^2 \quad (\text{A.14})$$

$$\frac{d[\text{SOD}]}{dt} = -k_{10} \cdot \bar{\kappa}_{\text{SOD}}^* \cdot \bar{G} \cdot [\text{SOD}]^2 \quad (\text{A.15})$$

Integrating the Eqs. (A.14) and (A.15) from time $t = 0$ (initial concentrations of enzymes, $[\text{CAT}]_0$ and $[\text{SOD}]_0$) to an instant time t ($[\text{CAT}]$ and $[\text{SOD}]$):

$$[\text{CAT}] = \frac{1}{1/[\text{CAT}]_0 + k_9 \cdot \bar{\kappa}_{\text{CAT}}^* \cdot \bar{G} \cdot t} \quad (\text{A.16})$$

$$[\text{SOD}] = \frac{1}{1/[\text{SOD}]_0 + k_{10} \cdot \bar{\kappa}_{\text{SOD}}^* \cdot \bar{G} \cdot t} \quad (\text{A.17})$$

Finally, the reaction rate of the bacteria inactivation is obtained from the kinetic of Eq. (T.13) and the mass balance of the bacteria in the reactor.

$$\frac{d[B_v]}{dt} = -k_{13}[\text{HO}^\bullet][\text{O}_2^-][B_v] \quad (\text{A.18})$$

Introducing Eqs. (A.4) and (A.6) into (A.18), the following expression is obtained:

$$\frac{d[B_v]}{dt} = -k_{13} \cdot \frac{2\gamma_3[\text{H}_2\text{O}_2]}{k_6[\text{H}_2\text{O}_2] + k_{11}} \cdot \frac{\gamma_1 + \gamma_2 \cdot e_{\text{NADH}}^a}{k_3[\text{SOD}] + k_{12}} \cdot [B_v] \quad (\text{A.19})$$

References

- [1] K.G. McGuigan, R.M. Conroy, H.-J. Mosler, M. du Preez, E. Ubomba-Jaswa, P. Fernandez-Iba ez, Solar water disinfection (SODIS): a review from bench-top to roof-top, *J. Hazard. Mater.* 235–236 (2012) 29–46.
- [2] R.M. Conroy, M. Elmore-Meegan, T. Joyce, K.G. McGuigan, J. Barnes, Solar disinfection of drinking water and diarrhoea in Maasai children: a controlled field trial, *Lancet* 348 (1996) 1695–1697.

- [3] R.M. Conroy, M.E. Meegan, T. Joyce, K. McGuigan, J. Barnes, Solar disinfection of water reduces diarrhoeal disease: an update, *Arch. Dis. Child.* 81 (1999) 337–338.
- [4] R.P. Sinha, D.-P. H der, UV-induced DNA damage and repair: a review, *Photochem. Photobiol. Sci.* 1 (2002) 225–236.
- [5] R.M. Tyrrell, S.M. Keyse, New trends in photobiology the interaction of UVA radiation with cultured cells, *J. Photochem. Photobiol. B* 4 (1990) 349–361.
- [6] A.L. Santos, V. Oliveira, I. Baptista, I. Henriques, N.C.M. Gomes, A. Almeida, A. Correia, A. Cunha, Wavelength dependence of biological damage induced by UV radiation on bacteria, *Arch. Microbiol.* 195 (2013) 63–74.
- [7] M. Berney, H.-U. Weilenmann, T. Egli, Flow-cytometric study of vital cellular functions in *Escherichia coli* during solar disinfection (SODIS), *Microbiology* 152 (2006) 1719–1729.
- [8] M. Berney, H.-U. Weilenmann, A. Simonetti, T. Egli, Efficacy of solar disinfection of *Escherichia coli*, *Shigella flexneri*, *Salmonella typhimurium* and *Vibrio cholera*, *J. Appl. Microbiol.* 101 (2006) 828–836.
- [9] P.M. Oates, P. Shanahan, M.F. Polz, Solar disinfection (SODIS): simulation of solar radiation for global assessment and application for point-of-use water treatment in Haiti, *Water Res.* 37 (2003) 47–54.
- [10] O.K. Dalrymple, E. Stefanakos, M.A. Trotz, D.Y. Goswami, A review of the mechanisms and modeling of photocatalytic disinfection, *Appl. Catal. B* 98 (2010) 27–38.
- [11] J. Marug n, R. van Grieken, A.E. Cassano, O.M. Alfano, Intrinsic kinetic modeling with explicit radiation absorption effects of the photocatalytic oxidation of cyanide with TiO₂ and silica-supported TiO₂ suspensions, *Appl. Catal. B* 85 (2008) 48–60.
- [12] J. Marug n, R. van Grieken, C. Pablos, M.L. Satuf, A.E. Cassano, O.M. Alfano, Rigorous kinetic modelling with explicit radiation absorption effects of the photocatalytic inactivation of bacteria in water using suspended titanium dioxide, *Appl. Catal. B* 102 (2011) 404–416.
- [13] J.N. Jensen, Disinfection model based on excess inactivation sites: implications for linear disinfection curves and the Chick-Watson dilution coefficient, *Environ. Sci. Technol.* 44 (2010) 8162–8168.
- [14] L.T. Fan, A. Argoti, Nonlinear stochastic model for bacterial disinfection: analytical solution and Monte Carlo simulation, *Ind. Eng. Chem. Res.* 51 (2012) 1697–1702.
- [15] J. Visick, S. Clarke, RpoS- and OxyR-independent induction of HPI catalase at stationary phase in *Escherichia coli* and identification of *rpoS* mutations in common laboratory strains, *J. Bacteriol.* 179 (13) (1997) 4158–4163.
- [16] J.A. Imlay, I. Fridovich, Assay of metabolic superoxide production in *Escherichia coli*, *J. Biol. Chem.* 266 (11) (1991) 6957–6965.
- [17] L.C. Seaver, J.A. Imlay, Are respiratory enzymes the primary sources of intracellular hydrogen peroxide?, *J. Biol. Chem.* 279 (47) (2004) 48742–48750.
- [18] M. Tanaka, K. Ohkubo, S. Fukuzumi, DNA cleavage by UVA irradiation of NADH with dioxygen via radical chain processes, *J. Phys. Chem. A* 110 (2006) 11214–11218.
- [19] J.A. Imlay, Cellular defenses against superoxide and hydrogen peroxide, *Annu. Rev. Biochem.* 77 (2008) 4.1–4.22.
- [20] S.X. Chen, P. Schopfer, Hydroxyl-radical production in physiological reactions, *Eur. J. Biochem.* 260 (3) (1999) 726–735.
- [21] F. Joubert, H.M. Fales, H. Wen, C.A. Combs, R.S. Balaban, NADH enzyme-dependent fluorescence recovery after photobleaching (ED-FRAP): applications to enzyme and mitochondrial reaction kinetics, *in vitro*, *Biophys. J.* 86 (2004) 629–645.
- [22] A.S. Gort, J.A. Imlay, Balance between endogenous superoxide stress and antioxidant defenses, *J. Bacteriol.* 180 (6) (1998) 1402–1410.
- [23] P. Viglino, M. Scarpa, F. Coin, G. Rotilio, A. Rigo, Oxidation of reduced Cu, Zn superoxide dismutase by molecular oxygen. A kinetic study, *Biochem. J.* 237 (1986) 305–308.
- [24] I.A. Abreu, D.E. Cabelli, Superoxide dismutases – a review of the metal-associated mechanistic variations, *Biochim. Biophys. Acta* 2010 (1804) 263–274.
- [25] J.A. Imlay, Pathways of oxidative damage, *Annu. Rev. Microbiol.* 57 (2003) 395–418.
- [26] G.V. Buxton, C.L. Greenstock, W.P. Helman, A.B. Ross, Critical review of rate constants for reactions of hydrated electrons, hydrogen atoms and hydroxyl radicals ($\cdot\text{OH}/\cdot\text{O}^-$) in aqueous solution, *J. Phys. Chem. Ref. Data* 17 (1988) 513–886.
- [27] H. Gallard, J. De Laat, Kinetic modelling of Fe(III)/H₂O₂ oxidation reactions in dilute aqueous solution using atrazine as a model organic compound, *Water Res.* 34 (2000) 3107–3116.
- [28] M.J. Flores, R.J. Brandi, A.E. Cassano, M.D. Labas, Chemical disinfection with H₂O₂ – the proposal of a reaction kinetic model, *Chem. Eng. J.* 198–199 (2012) 388–396.
- [29] C.S. Zalazar, M.D. Labas, R.J. Brandi, A.E. Cassano, Dichloroacetic acid degradation employing hydrogen peroxide and UV radiation, *Chemosphere* 66 (2007) 281–286.
- [30] H.U. Bergmeyer, Enzymes 1: oxidoreductases, transferases, *in: Methods of Enzymatic Analysis*, third ed., vol. 3, VCH Publ., Weinheim, 1983, pp. 274–277.
- [31] Z. Tao, R.A. Raffel, A.-K. Souid, J. Goodisman, Kinetic studies on enzyme-catalyzed reactions: oxidation of glucose, decomposition of hydrogen peroxide and their combination, *Biophys. J.* 96 (2009) 2977–2988.
- [32] L.C. Seaver, J.A. Imlay, Alkyl hydroperoxide reductase is the primary scavenger of endogenous hydrogen peroxide in *Escherichia coli*, *J. Bacteriol.* 183 (24) (2001) 7173–7181.
- [33] L.C. Seaver, J.A. Imlay, Hydrogen peroxide fluxes and compartmentalization inside growing *Escherichia coli*, *J. Bacteriol.* 183 (24) (2001) 7182–7189.
- [34] G. Maria, M.D. Ene, I. Jipa, Modelling enzymatic oxidation of d-glucose with pyranose 2-oxidase in the presence of catalase, *J. Mol. Catal. B* 74 (3–4) (2012) 209–218.
- [35] O. Idil, C. Darcan, T. Ozen, R. Ozkanca, The effect of UV-A and various visible light wavelengths radiations on expression level of *Escherichia coli* oxidative enzymes in seawater, *Jundishapur J. Microbiol.* 6 (3) (2013) 230–236.
- [36] H.-D. Youn, Y.-I. Yim, K. Kim, Y.C. Hah, S.-O. Kang, Spectral characterization and chemical modification of catalase-peroxidase from streptomyces sp., *J. Biol. Chem.* 270 (3) (1995) 13740–13747.
- [37] F. Bosshard, K. Riedel, T. Schneider, C. Geiser, M. Bucheli, T. Egli, Protein oxidation and aggregation in UVA-irradiated *Escherichia coli* cells as signs of accelerated cellular senescence, *Environ. Microbiol.* 12 (11) (2010) 2931–2945.
- [38] D. Spuhler, J.A. Rengifo-Herrera, C. Pulgarin, The effect of Fe²⁺, Fe³⁺, H₂O₂ and the photo-Fenton reagent at near neutral pH on the solar disinfection (SODIS) at low temperatures of water containing *Escherichia coli* K12, *Appl. Catal. B* 96 (2010) 126–141.
- [39] P. Fernandez-Ibanez, J.A. Byrne, M.I. Polo-Lopez, P.S.M. Dunlop, P. Karaolia, D. Fatta-Kassinos, Chapter 3. Solar photocatalytic disinfection of water, *in: D.D. Dionysiou, G. Li Puma, J. Ye, J. Schneider, D. Bahnemann (Eds.), RSC Energy and Environment Series No. 15 Photocatalysis: Applications*, 2016 (in press).
- [40] T.A. Jackson, A. Karapetian, A.-F. Miller, T.C. Brunold, Spectroscopic and computational studies of the azide-adduct of Manganese Superoxide Dismutase: definitive assignment of the ligand responsible for the low-temperature thermochromism, *J. Am. Chem. Soc.* 126 (2004) 12477–12491.
- [41] E. Nakamaru-Ogiso, M.-C. Kao, H. Chen, S.C. Sinha, T. Yagi, T. Ohnishi, The membrane subunit Nuol(ND5) is involved in the indirect proton pumping mechanism of *Escherichia coli* Complex I, *J. Biol. Chem.* 285 (50) (2010) 39070–39078.
- [42] I. Kishko, B. Harish, V. Zayats, D. Reha, B. Tenner, D. Beri, T. Gustavsson, R. Ettrich, J. Carey, Biphasic kinetic behavior of *E. coli* WrbA, an FMN-dependent NAD(P)H:quinone oxidoreductase, *PLoS One* 7 (8) (2012) 1–10.
- [43] D. Raes, P. Steduto, T.C. Hsiao, E. Fereres, Chapter 2. Users Guide, *in AquaCrop Version 4.0*, FAO, Land and Water Division, Rome, Italy, 2012.
- [44] F. Vatansever, W.C.M.A. de Melo, P. Avci, D. Vecchio, M. Sadasivam, A. Gupta, R. Chandran, M. Karimi, N.A. Parizotto, R. Yin, G.P. Tegos, M.R. Hamblin, Antimicrobial strategies centered around reactive oxygen species – bactericidal antibiotics, photodynamic therapy, and beyond, *Microbiol. Rev.* 37 (2013) 955–989.
- [45] J.D. Hoerter, A.A. Arnold, C.S. Ward, M. Sauer, S. Johnson, T. Fleming, A. Eisenstark, Reduced hydroperoxidase (HPI and HPII) activity in the Δfur mutant contributes to increased sensitivity to UVA radiation in *Escherichia coli*, *J. Photochem. Photobiol. B* 79 (2005) 151–157.